XLIII CILAMCE
21–25, November, 2022
FOZ DO IGUAÇU – PR – BRAZIL

Fission and Deformations in the Colon Epithelium using Finite Element Methods

G. Romanazzi[1], G. Settanni[2]

[1]*Dept. of Applied Mathematics, State University of Campinas, UNICAMP , Campinas, SP, Brazil*
roman@ime.unicamp.br
[2]*Dyrecta Lab, Istituto di Ricerca , Conversano, Italy*
giuseppina.settanni@dyrecta.com

Abstract. The goal of this work is to model and simulate a crypt deformation and fission in the colon epithelium originated by an abnormal cell proliferation located in the crypt walls.

Keywords: Colorectal Cancer, PDE System, Finite Element Method, Tissue Deformation

1 Introduction

Colorectal cancer is the third most common diagnosed cancer, and was the second cancer for death incidence World Health Organization [1]. The World Health Organization asserts that the economic impact of cancer is significant and increasing, in fact the total annual economic cost of cancer in 2010 was estimated at approximately US$ 1.16 trillion Stewart and Wild [2]. In the early nineties, many researchers investigated the origin of colorectal cancer and established the basis of a carcinogenesis theory that links cell mutations to cancer formation. As explained in Carulli et al. [3], Drasdo and Loeffler [4], Meineke et al. [5], experimental studies show that carcinogenesis starts in the intestinal crypts densely distributed along the colonic epithelium. The intestinal crypts, hereafter just called crypts, have a finger like structure closed at the bottom end and with an open orifice in the top superficial epithelium region in contact with the lumen. Stem, transit proliferative and fully differentiated cells are located in different positions along the crypt walls in a normal epithelium, that is without any abnormal cell. In particular, stem cells occupies the first third of the crypt height from its bottom, whereas transit proliferative cells (also called semi-differentiated cells) are mostly located between the first third and the second third of the crypt and fully differentiated cells are in the crypt top third, see Fig. 1. Moreover it is known that in a normal epithelium crypt, stem cells live and reside at the crypt bottom and that differentiation gives rise to transit proliferative cells that can migrate upwards in the direction of the top orifice. During this migration, transit cells continue to differentiate and become fully differentiated (or mature) at the crypt top. Meineke et al. [5], van Leeuwen et al. [6], Almet et al. [7].

The presence of deformed crypts can be considered a preliminary stage of malignant adenoma formation, and cell mutations due to an activation of Wnt signaling can be responsible for this abnormal crypt formation. In particular, aberrant crypt foci (ACF), defined as microscopic clusters of abnormal crypts, are believed to be the first stage of a formation of adenomatous polyps, see [8–10]. It is also known that human ACF have a hyperproliferative epithelium and their growth are mostly generated by abnormal crypt fission, see [11, 12]. Moreover, biological evidence confirms that colonic adenoma formation is characterized by cell proliferation at the top of the crypt and by a high index of crypt fission, see [13–15]. Hence, as introduced in [16], there exists a correlation between location of proliferative cells in the upper part of the crypt, aberrant crypt fission and adenoma formation. In this regard, [17] highlights that Wnt signaling may block cell differentiation suppressing some differentiation-specific genes, consequently an accumulation of proliferative cells happens in the crypt region between transit and differentiated cells. We model in this work this case, where some transit cells, unable to differentiate at the crypt top, crowd some crypt wall region leading to a pressure acting on crypt walls that can deform the crypt geometry up to obtain a complete fission.

This model permits to understand how abnormal cell location leads to morphological changes during the crypt fission, generating two new crypts. Specifically, we have the chance to use the model for predicting how the pattern of an histological colon image can evolve, determining direction and dimension of the adenoma growth.

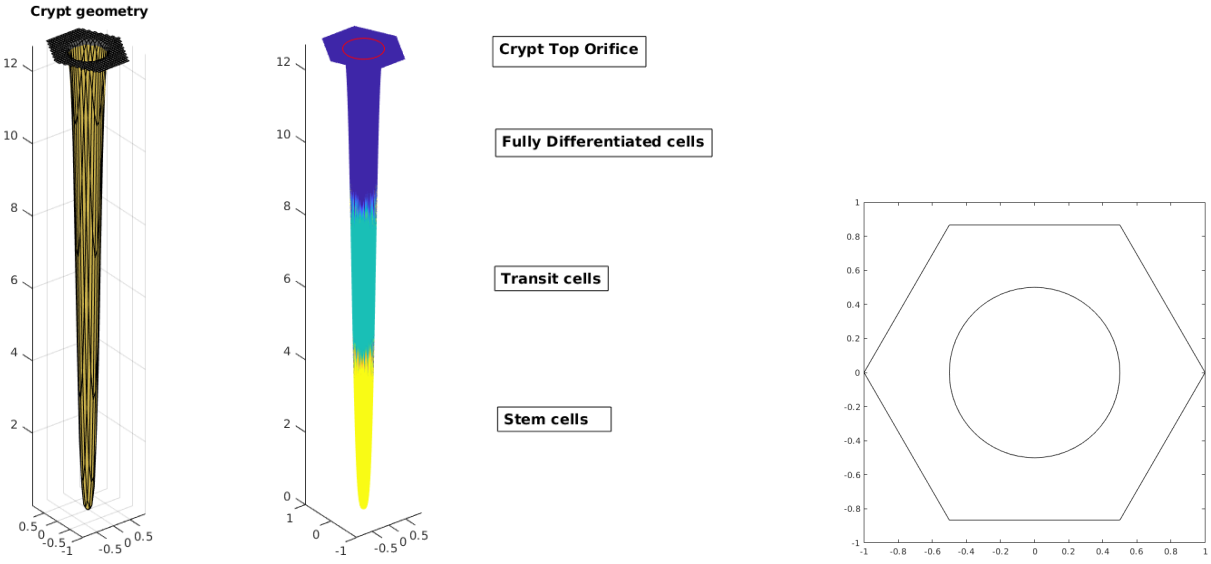

Figure 1. (a): Crypt domain Γ is a two dimensional manifold with a circular orifice. Along its walls are located three cell families. (b): Stem cells (in yellow) are located at the bottom, transit cells (in cyan) in the mid-crypt region and differentiated cells (in blue) in the top third of the crypt height. The circular crypt orifice has radius $R = 0.5$ marked in red and height $h = 12.7$.(c): Hexagonal crypt top orifice.

This can be significant for a disease prevention.

2 Crypt Domain and Mathematical Model

As done in Campos et al. [18], Figueiredo et al. [19] in order to model the cell dynamics in a crypt Γ, we denote by $c(x, y, z, t)$ the density of the stem and semi–differentiated cells located at $(x, y, z) \in \Gamma$ at time t. The semi–differentiated cells are under the effect of a cell-cell adhesion pressure $p(x, y, z, t)$, at $(x, y, z) \in \Gamma$ at time t, that is responsible for the cell migration. The crypt shape used is that illustrated in Fig. Fig. 1, that is almost a half prolate with the open orifice located in the intestinal lumen that is packed in a hexagonal distribution in the colon epithelium.

On averaging Guebel and Torres [12], a crypt has a height that is almost 12.7 times the diameter of the top crypt orifice, in particular, its height from the bottom to the top orifice is $433\mu m$ and the diameter of the top orifice is $34.1\mu_m$ including the epithelium tissue. After a proper scaling of its dimensions to have a orifice diameter $2R = 1$ we get for our crypt domain Γ a height $h = 12.7$ and a radius $R = 0.5$. We assume also that a crypt can be represented by a two dimensional manifold Γ defined by a continuum and differentiable function $f : \overline{\Omega} \to \mathbb{R}$, that is

$$\Gamma = \{(x, y, z) \in \mathbb{R}^3 : (x, y) \in \overline{\Omega}, z = f(x, y)\}, \tag{1}$$

where $\overline{\Omega}$ is an hexagon with edge length 1, centered in the origin $O = (0, 0)$, and f is the function

$$f(x, y) = h(1 - e^{-\left(\frac{R(x,y)}{\sigma}\right)^2}), \quad (x, y) \in \overline{\Omega}, \tag{2}$$

with $R(x, y) = (x - 1/2)^2 + (y - 1/2)^2$, and $\sigma > 0$. In the following we use $\sigma = 0.1$ that guarantees to have a circular orifice with radius $R = 0.5$, see Fig. 1.

Now considering the mathematical model for the colon cell dynamics presented in Campos et al. [18], Figueiredo et al. [19],the behavior of the colon cell density c and pressure p can be described by the following IBVP written in the crypt manifold Γ

$$\begin{cases} -\xi \Delta_\Gamma p = \alpha c, \\ \dfrac{\partial c}{\partial t} - \nabla_\Gamma \cdot (\xi c \nabla_\Gamma p) = \nabla_\Gamma \cdot (D \nabla_\Gamma c) + \beta c, \ \text{in } \Gamma \times (0, T], \\ p = c = 0, \quad \text{on } \partial\Gamma \times (0, T], \\ c(0) = c_0, \quad \text{in } \Gamma, \end{cases} \tag{3}$$

where the diffusion coefficient D is supposed constant, and ξ is a positive constant that depends on the permeability and viscosity of the epithelium tissue Figueiredo et al. [19]. The cell velocity v in (3) is given by Darcy's law $v = -\xi\nabla_\Gamma p$. Here the operators ∇_Γ and Δ_Γ are the gradient and Laplace operators acting on the spatial variables x, y, z on the crypt manifold Γ. In (3), the function c_0 describes the initial cell density in the crypt, α is the proliferation rate for the stem and transit cells, and β is defined by $\beta = \alpha - \gamma$, where γ denotes the rate of transformation of the transit cells into fully differentiated cells. In a normal epithelium crypt, γ is supposed null in the crypt bottom where no transit cells are present and increases along the crypt axis up to two thirds of its height where thereafter only mature cells lives Drasdo and Loeffler [4], Potten et al. [20], and therefore it can be considered null also in the last third of the crypt axis. We use for our crypt domain a function γ that is an approximation of that computed in [18] and whose plot is given in Fig. 2.

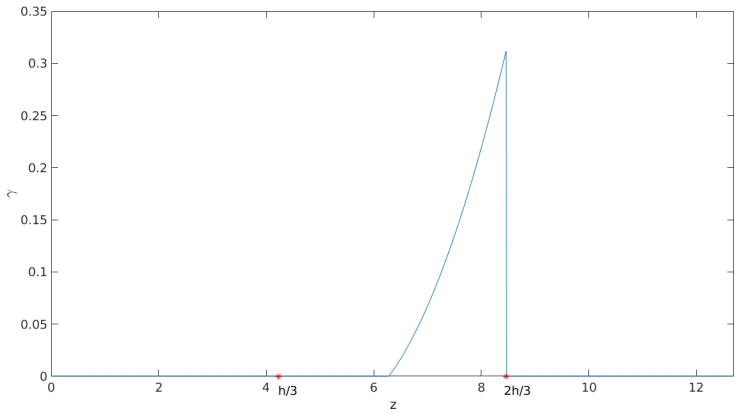

Figure 2. Rate of transformation of transit cells into fully differentiated, $\gamma = \gamma(z)$, depends only on the crypt quote z. It is active and positive only in the transit cells region. $z \in [\frac{h}{3}, 2\frac{h}{3}]$.

Also the normal proliferation rate α^*, see Fig. 3, depends only on the crypt quote z as described in Campos et al. [18] and is given in the normal epithelium by

$$\alpha^*(z) = \begin{cases} \tau\left(1 - \dfrac{z}{\frac{1}{3}h}\right)^2 \left(1 - \dfrac{z}{\frac{2}{3}h}\right)^2 e^{-\left(1-\frac{z}{\frac{1}{3}h}\right)^2}, & \text{if } \dfrac{h}{3} \le z \le \dfrac{2}{3}h \\ 0, & \text{if } \dfrac{2}{3}h < z \le h \text{ or } 0 \le z < \dfrac{h}{3}, \end{cases} \tag{4}$$

In (4) $\tau = 3.5468$ is a constant that guarantees that in the normal epithelium the cell velocity due to the cell-cell adhesion pressure $v = -\xi\nabla_\Gamma p$ for $\xi = 0.02473$ (used in Campos et al. [18]) reaches its maximum v_{max} at the crypt quote $z = \frac{2}{3}h$ with a value corresponding to 0.85 cell positions per hour. In our rescaled geometry this corresponds to $vmax = 0.85 * h_{cell} \approx 0.147067$,where $h_{cell} \approx 0.1730$ is the height average of the transit cell in a our crypt of height $h = 12.7$.

In order to simulate an abnormal proliferation that leads to a deformation of the orifice and a possible fission we add a Gaussian term to α^* acting on the top third of the crypt height obtaining the proliferation rate α:

$$\alpha(z) = \alpha^*(z) + d_1 e^{-((x-x_{abn})^2 + (y-y_{abn})^2)/d_2} \tag{5}$$

whose plot is shown in Fig. 4. α defined in (5) is used in the PDE system (3).

This system is equivalent to the following PDE system written in the domain $\bar{\Omega} \times (0, T]$

$$\begin{cases} -\nabla \cdot (\xi\mathcal{A}\nabla p) = \sqrt{det(G)}\alpha c, \\ \sqrt{det(G)}\dfrac{\partial c}{\partial t} - \nabla \cdot (\xi\mathcal{A}\nabla pc) = \nabla \cdot (D\mathcal{A}\nabla c) + \sqrt{det(G)}\beta c, \text{ in } \Omega \times (0, T] \\ c = p = 0 \text{ on } \partial\Omega \times (0, T], \\ c(0) = \tilde{c}_0 \text{ in } \Omega, \end{cases} \tag{6}$$

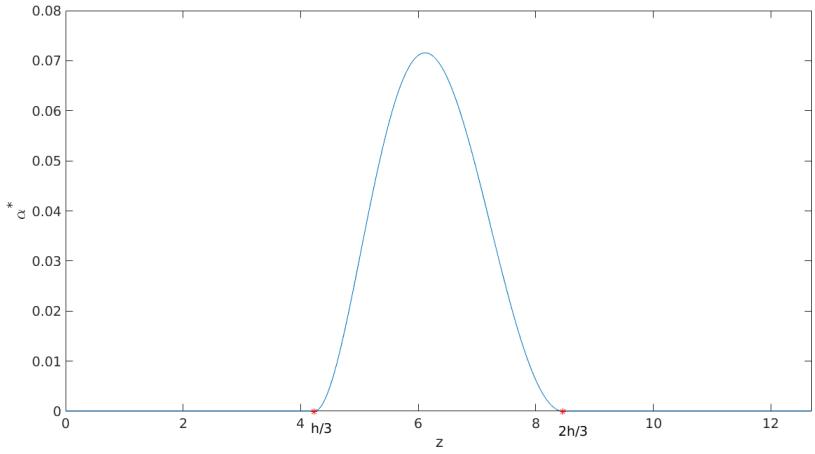

Figure 3. Proliferation rate α^* of stem and transit cells in a normal epithelium crypt along its vertical axis.

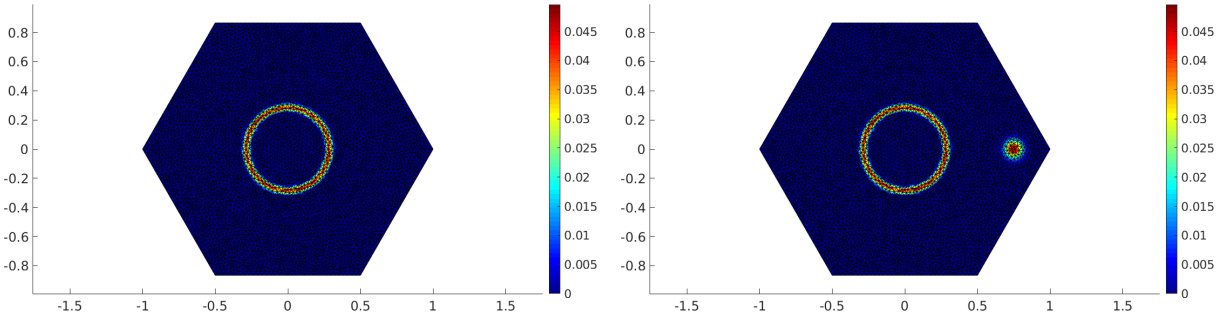

(a) (b)

Figure 4. Proliferation rates:(a) normal α^* and (b) abnormal α, plotted in the manifold crypt domain $\bar{\Omega}$, defined respectively in (4) and (5) for $\tau = 3.5468$, $d_1 = 0.05$, $d_2 = 0.00375$.

where

$$G = \begin{bmatrix} 1 + (\dfrac{\partial f}{\partial x})^2 & \dfrac{\partial f}{\partial x}\dfrac{\partial f}{\partial y} \\ \dfrac{\partial f}{\partial x}\dfrac{\partial f}{\partial y} & 1 + (\dfrac{\partial f}{\partial y})^2 \end{bmatrix}, \quad \mathcal{A} = \frac{1}{\sqrt{det(G)}} \begin{bmatrix} 1 + \left(\dfrac{\partial f}{\partial y}\right)^2 & -\dfrac{\partial f}{\partial x}\dfrac{\partial f}{\partial y} \\ -\dfrac{\partial f}{\partial x}\dfrac{\partial f}{\partial y} & 1 + \left(\dfrac{\partial f}{\partial x}\right)^2 \end{bmatrix}.$$

An example of initial transit cell density c_0 that presents abnormal cells at the crypt top is given in Fig. 5.

3 Modeling the abnormalities: cell proliferation, crypt deformation and fission

An abnormal proliferation of cells in the crypt or similarly a modification of the Wnt signaling Figueiredo et al. [19], Romanazzi and Settanni [21] are responsible, as described in the Introduction, for the deformation of the crypt walls that can evolve up to a complete fission in our modeling. In order to force an abnormal proliferation we suppose in our simulations an initial cell distribution with proliferative cells located also over the two third of the crypt height. This can be obtained by using for instance the proliferation rate defined in (5), plotted in Fig. 4, (b), and the initial cell density plotted in Fig. 5.

As done in [19], we suppose that the epithelium has a visco-elastic structure with viscosity acting only at the top orifice and that the deformations are due to the force $f = -\xi\nabla(p - p^*)$ where p^* is the cell-cell adhesion pressure in a normal crypt. This leads to a displacement u of the top orifice that in a quasi-static regime is obtained by solving the equilibrium relation

$$-\nabla \cdot \sigma(u) = f, i = 1, 2$$

where $\sigma(u) = \sigma_{ij}(u)$ is a Cauchy stress tensor. The deformation associated to this displacement is applied only in the crypt top orifice as done in Figueiredo et al. [19], with the only difference that this force f is obtained by

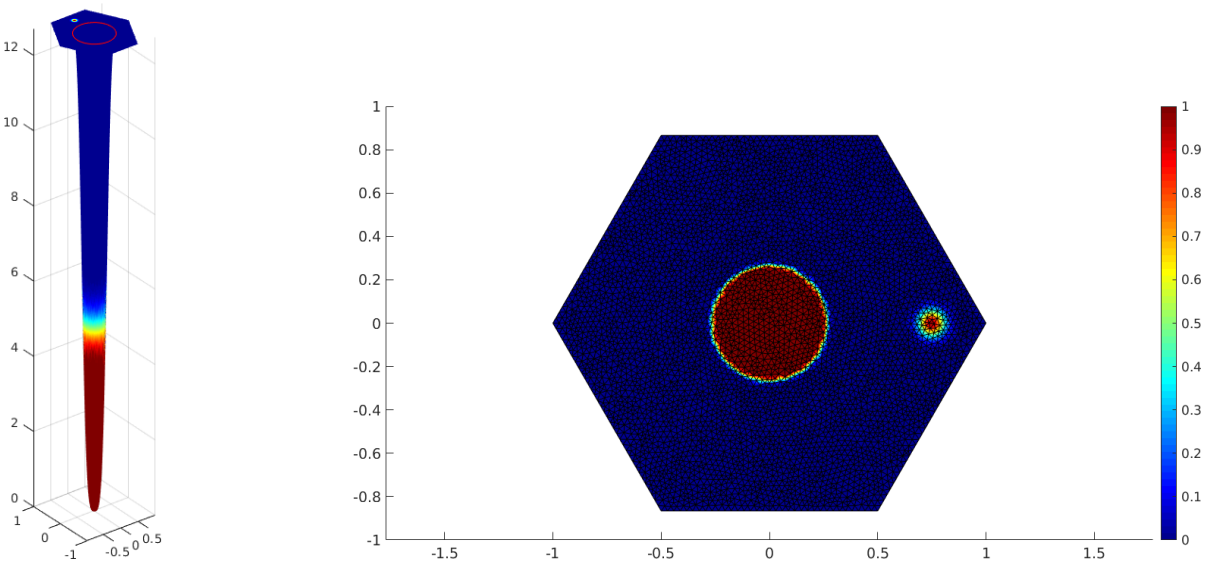

(a) (b)

Figure 5. Initial cell density c0: (a) in the manifold crypt domain Γ; (b) in the parametrized hexagonal crypt domain $\bar{\Omega}$. Note that abnormal cells are located at the crypt top.

using the difference of pressure $p - p^*$ measured in the manifold PDE model (6) in a region that corresponds to the vertical dimension (cell height) rather than along its width half dimension.

4 Variational formulation and finite elements method

The PDE system (6) is solved numerically by using a Galerkin piecewise linear finite element method. In order to build it we analyze the variational formulation of (6) in
$V_h = \{v \in C(\overline{\Omega}(t))|\forall K \in \mathcal{T}_h \; v|_K$ piecewise linear, $v|_{\partial\Omega} = 0\}$ with basis $\{\phi_k\}_{k=1,\ldots,N_{nodes}}$ formed by bounded piecewise linear functions in the triangulation $\mathcal{T}_h = \{T_l\}_{l=1,\ldots,N_{triang}}$ of $\bar{\Omega}(t)$ where N_{triang} is the number of triangles of $\mathcal{T}_h$ and N_{nodes} is the number of the internal nodes of $\mathcal{T}_h$. This variational formulation can be read as follows: find c, p in the time interval $[t_{n-1}, t_n]$ such that for each basis function ϕ_k of V_h

$$\int_{\bar{\Omega}(t)} \xi \sum_{i,j} \mathcal{A}_{i,j} \frac{\partial p}{\partial x_j} \frac{\partial w_k}{\partial x_i} dx = \int_{\bar{\Omega}(t)} \alpha c \phi_k dx$$

and

$$\int_{\bar{\Omega}(t)} \frac{\partial c}{\partial t} \phi_k dx + \int_{\bar{\Omega}(t)} \xi \sum_{i,j} \mathcal{A}_{i,j} \frac{\partial p}{\partial x_j} c \frac{\partial w_k}{\partial x_i} dx + \int_{\bar{\Omega}(t)} \xi \sum_{i,j} \mathcal{A}_{i,j} \frac{\partial c}{\partial x_j} \frac{\partial w_k}{\partial x_i} dx = \int_{\bar{\Omega}(t)} \beta c \phi_k dx$$

where $w_k = \dfrac{\phi_k}{\sqrt{\det g}}$. Now using the first order Backward Euler method in the time interval $[t_n, t_{n+1}]$ of time-step Δ_t the method reduces to: find $\mathbf{p}^{h,n}$,$\mathbf{c}^{h,n}$, the approximate numerical solutions of (6) at time t_n, that satisfy

$$\begin{aligned} &G_\xi \mathbf{p}^{h,n} = \mathbf{M}_\alpha c^{h,n}, \\ &(\mathbf{M}_1 + \mathbf{\Delta}_t (D_{\nabla_p} + G_1)) \mathbf{c}^{h,n} = \mathbf{M}_\beta \mathbf{c}^{h,n-1}, \end{aligned} \tag{7}$$

where

$$\mathbf{G}_a = \left(\int_{\bar{\Omega}(t)} a \nabla w_k \cdot (A \nabla \phi_l) \, dx \right)_{k,l=1,2}, \; \mathbf{M}_a = \left(\int_{\bar{\Omega}(t)} a(x) \phi_k \phi_l dx \right)_{k,l=1,2}, \; \mathbf{D}_{\nabla p} = \left(\int_{\bar{\Omega}(t)} (\tilde{\mathbf{d}} \cdot \nabla \phi_k) \phi_l \right)_{k,l}$$

with $\tilde{\mathbf{d}} = \mathbf{p}^{h,n-1} \cdot (\mathcal{A} \nabla \phi_k)_{k=1,\ldots,N_{nodes}}$. The linear systems (7) are solved in sequence for $n = 0, 1, 2, \ldots$ starting by the first system to get $p^{h,0}$ associated to a known initial condition $c^{h,0}$, and obtaining $c^{h,1}$ from the second linear

system, then we obtain $p^{h,1}$ from the first linear system and so on. We solve these systems by using the Matlab *mldivide* numerical algebra routine MATLAB [22]. An example of pressure solution $p^{h,n}$ of the finite element method on the triangularized domain $\Omega_h = \cup_{K \in \mathcal{T}_h} K$ is shown in Fig. 6.

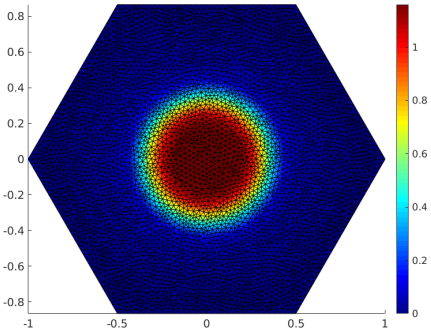

Figure 6. Pressure $p^{h,n}$ in the triangularized domain Ω_h.

5 Fission and crypt deformation

The novelty of this work with respect previous authors works is in the orifice deformation that can now evolve up to a complete continuum fission of the crypt, see Fig. 7.

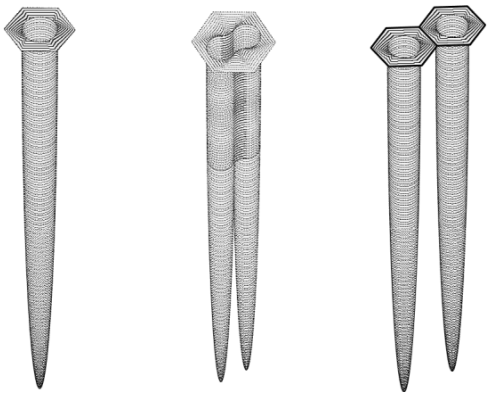

Figure 7. Fission steps of a crypt. Left: normal crypt. Center: deformed crypt. Right: complete fission.

In fact in our new methodology we allow to step forward from a deformed crypt to a fission. This happens when we measure a sufficient high curvature of the crypt orifice in a crypt region over the two thirds of the crypt where we find that cell density c passes the limit value of $c = 0.8$. Note that this c value is the same of that used in Romanazzi and Settanni [21] for proceeding to a complete fission. Here the curvature $k(s)$ of the crypt orifice formed by the points $(x(s), y(s))$ with s in a bounded interval I_k is measured by using the curvature formula

$$k(s) = \frac{x'(s)y''(s) - y'(s)x''(s)}{(x'^2(s) + y'^2(s))^{\frac{3}{2}}} \tag{8}$$

$k(s)$ is numerically approximated replacing the centered second order finite difference method in each derivative term in (8) as done in Dunn et al. [23].

6 Conclusions

We presented a new numerical methodology based on finite element methods and biological information that allows to simulate the first stage of carcinogenesis in the colon originated by abnormal crypt cell proliferation. The methodology couples the fission discrete model presented in Romanazzi and Settanni [21] with the continuous crypt deformation model Figueiredo et al. [19], where the cell dynamics model is approximated by using a piecewise linear finite element method on a bidimensional crypt manifold representation as that used in Campos et al. [18]. This allows to have a novel continuous deformation-fission model that starting with a normal crypt

presenting an abnormal cell proliferation in a localized region can deform its crypt orifice and evolve continuously to a complete fission.

Authorship statement. The authors hereby confirm that they are the sole liable persons responsible for the authorship of this work, and that all material that has been herein included as part of the present paper is either the property (and authorship) of the authors, or has the permission of the owners to be included here.

References

[1] World Health Organization. Cancer. `http://www-cs-faculty.stanford.edu/~{}uno/abcde.html`. Accessed 20 November 2018, 2018.

[2] B. W. Stewart and C. P. Wild. *World cancer report 2014*. International Agency for Research on Cancer, Lyon, 2014.

[3] A. J. Carulli, L. C. Samuelson, and S. Schnell. Unraveling intestinal stem cell behavior with models of crypt dynamics. *Integr Biol (Camb)*, vol. 6, pp. 243–257, 2014.

[4] D. Drasdo and M. Loeffler. Individual-based models to growth and folding in one-layered tissues: intestinal crypts and early development. *Nonlinear Anal-Theor*, vol. 47, pp. 245–256, 2001.

[5] F. A. Meineke, C. S. Potten, and M. Loeffler. Cell migration and organization in the intestinal crypt using a lattice-free model. *Cell Prolif*, vol. 34, pp. 253–266, 2001.

[6] I. M. M. van Leeuwen, H. M. Byrne, O. E. Jensen, and J. R. King. Crypt dynamics and colorectal cancer: advances in mathematical modelling. *Cell Prolif*, vol. 39, pp. 157–181, 2006.

[7] A. A. Almet, B. D. Hughes, K. A. Landman, I. S. Näthke, and J. M. Osborne. A multicellular model of intestinal crypt buckling and fission. *Bull Math Biol*, vol. 80, pp. 335–359, 2018.

[8] L. Roncucci, M. Pedroni, F. Vaccina, P. Benatti, L. Marzona, and A. De Pol. Aberrant crypt foci in colorectal carcinogenesis. cell and crypt dynamics. *Cell Prolif*, vol. 33, pp. 1–18, 2000.

[9] T. Tanaka. Colorectal carcinogenesis: review of human and experimental animal studies. *J Carcinog*, vol. 8, pp. 5–23, 2009.

[10] M. J. Wargovich, V. R. Brown, and J. Morris. Aberrant crypt foci: the case for inclusion as a biomarker for colon cancer. *Cancers*, vol. 2, pp. 1705–1716, 2010.

[11] K. Otori, K. Sugiyama, T. Hasebe, S. Fukushima, and H. Esumi. Emergence of adenomatous aberrant crypt foci (ACF) from hyperplastic ACF with concomitant increase in cell proliferation. *Cancer Res*, vol. 55, pp. 4743–4746, 1995.

[12] D. V. Guebel and N. V. Torres. A computer model of oxygen dynamics in human colon mucosa: Implications in normal physiology and early tumor development. *J Theor Biol*, vol. 250, pp. 389–409, 2008.

[13] B. M. Boman and J. Z. Fields. An APC:WNT counter-current-like mechanism regulates cell division along the human colonic crypt axis: a mechanism that explains how APC mutations induce proliferative abnormalities that drive colon cancer Development. *Front Oncol*, vol. 3, pp. 244, 2013.

[14] M. van De Wetering, E. Sancho, C. Verweij, W. De Lau, I. Oving, A. Hurlstone, K. Van Der Horn, E. Batlle, D. Coudreuse, A. P. Haramis, M. Tjon-Pon-Fong, P. Moerer, M. Van Den Born, G. Soete, S. Pals, M. Eilers, R. Medema, and H. Clevers. The β-catenin/TCF-4 complex imposes a crypt progenitor phenotype on colorectal cancer cells. *Cell*, vol. 111, pp. 241–250, 2002.

[15] S. Y. Wong, N. Mandir, R. A. Goodlad, B. C. Y. Wong, S. B. Garcia, S. K. Lam, and N. A. Wright. Histogenesis of human colorectal adenomas and hyperplastic polyps: the role of cell proliferation and crypt fission. *Gut*, vol. 50, pp. 212–217, 2002.

[16] H. S. Wasan, H. S. Park, K. C. Liu, N. K. Mandir, A. Winnet, P. Sasieni, W. F. Bodmer, R. A. Goodlad, and N. A. Wright. Colonic crypt organization and tumorigenesis. *J Pathol*, vol. 185, pp. 246–255, 1998.

[17] H. Clevers and R. Nusse. Wnt β-catenin signaling and disease. *Cell*, vol. 149, pp. 1192–1205, 2012.

[18] G. Campos, J. Ferreira, and G. Romanazzi. Density-pressure ibvp: numerical analysis, simulation and cell dynamics in a colonic crypt. *Applied Mathematics and Computation*, vol. 424, n. 127037, 2022.

[19] I. N. Figueiredo, C. Leal, G. Romanazzi, and B. Engquist. Biomathematical model for simulating abnormal orifice patterns in colonic crypts. *Math Biosci*, vol. 315, pp. 108221, 2019.

[20] C. S. Potten, C. Booth, and D. M. Pritchard. The small intestine as a model for evaluating adult tissue stem cell drug targets. *Int. J. Exp. Pathol.*, vol. 36, pp. 219–129, 2003.

[21] G. Romanazzi and G. Settanni. Mathematical model for simulation of morphological changes associated to crypt fission in the colon. *Discrete and Continuous Dynamical Systems Series S*, vol. , 2022.

[22] MATLAB. *version 9.4.0 (R2018a)*. The MathWorks Inc., Natick, Massachusetts, 2018.

[23] S. J. Dunn, P. L. Appleton, S. A. Nelson, I. S. N$'$athke, D. J. Gavaghan, and J. M. Osborne. A two-dimensional model of the colonic crypt accounting for the role of the basement membrane and pericryptal fibroblast sheath. *PLoS Comput Biol*, vol. 8, pp. e1002515, 2012.